

Effect of deconfinement on resonant transport in quantum wires

A. Ramšak

*J. Stefan Institute, SI-1000 Ljubljana, Slovenia
and Faculty of Mathematics and Physics, University of Ljubljana, SI-1000 Ljubljana, Slovenia*

T. Rejec

J. Stefan Institute, SI-1000 Ljubljana, Slovenia

J. H. Jefferson

*Defence Evaluation and Research Agency, Electronic Sector, St. Andrews Road, Great Malvern, Worcestershire WR14 3PS,
United Kingdom*

(Received 26 March 1998)

The effect of deconfinement due to finite band offsets on transport through quantum wires with two constrictions is investigated. It is shown that the increase in resonance linewidth becomes increasingly important as the size is reduced and ultimately places an upper limit on the energy (temperature) scale for which resonances may be observed. [S0163-1829(98)07231-2]

I. INTRODUCTION

Recent technological advances have enabled semiconductor nanostructures to be fabricated with feature sizes down to tens of angstroms. Such structures include arrays of “self-organized” quantum dots and quantum wires. The former are grown by heteroepitaxial deposition in which the overlayer material has the larger lattice parameter and forms quantum dots to relieve elastic strain.¹⁻⁷ The latter may be achieved by heteroepitaxial growth on “v”-groove surfaces, produced by optical lithography and etching, for which the overlayer atoms diffuse preferentially towards the base of groove producing a quantum wire with a crescent-shaped cross section.⁸⁻¹⁰ These structures have potential optoelectronic applications, such as light-emitting diodes, low-threshold lasers, and single-electron devices.

In this paper we consider the ballistic transport of electrons through quantum wires in which there are two constrictions defining a small region of quasiconfinement. Such a system can have a rich and complex resonance structure.¹¹⁻¹⁵ It has been investigated in detail by Nakazato and Blaikie,¹¹ who consider characteristic sizes down to ~ 100 nm and assume that the quantum wire is defined by infinitely high barriers. Such an assumption is reasonable provided that the resonance levels considered are at sufficiently low energy, i.e., somewhat lower than that of the real band edge in wider-gap material of the heterojunction. For the wire geometry they consider, the resonances are very sharp at $T=0$. Interchannel (mode) mixing of the electron waves is important for higher-order resonances and can give rise to unusual effects such as antiresonances. At these length scales, however, the possible observation of such resonances would be restricted to very low temperatures, where they would be easily swamped by defects and disorder.

The main purpose of the present work is to investigate the resonance structure for very narrow wires for which the energy (temperature) scale is higher and may even approach room temperature. Such a possibility is, of course, extremely important for device applications. As the size shrinks, the effect of a finite barrier for an electron in the wire becomes

increasingly relevant, the main effect being to broaden the resonances and restrict their number. Indeed, for a sufficiently small confining region, only a single isolated resonance level remains, with a continuum at higher energies. The increasing width of the resonance level is due to deconfinement of the electron wave function into the classically forbidden region beyond the potential step. However, all energies increase with increasing confinement and the important criterion is whether the lowest resonance peak can be resolved from the next resonance peak (or the continuum), which sets the temperature scale. To be specific, we shall, in what follows, mainly consider two-dimensional structures with a conduction-band offset of 0.4 eV, which is approximately the maximum offset in the conduction band (direct gap) for GaAs wires on an $\text{Al}_x\text{Ga}_{1-x}\text{As}$.

II. MODEL AND METHOD

For simplicity, we restricted the model to two dimensions with confinement in the y direction and propagating in the x direction. The wire shapes under consideration are symmetric around the x axis and shown in Fig. 1. The width of the wire is parametrized as $a(x) = a_0 - a_1 \sin^2 2\pi x/a_2$ for $0 \leq x \leq a_2$ and $a(x) \equiv a_0$ otherwise. For comparison we choose two generic geometries. In Fig. 1(a) the confined region is only weakly coupled to the “leads” and we thus expect strong (narrow) resonances. This structure is expected to behave in a similar way to a quantum dot, which is separated from its leads by tunnel barriers. On the other hand, for the geometry of Fig. 1(b), the constrictions are much smaller, resembling a wire with weak thickness fluctuations.

We model further the wire as two regions of constant potentials, $V=0$ within the wire “boundary,” and confining potential $V=V_0>0$ outside the wire. The corresponding two-dimensional Schrödinger equation reads

$$-\frac{\hbar^2}{2m^*} \left(\frac{\partial^2}{\partial x^2} + \frac{\partial^2}{\partial y^2} \right) \Psi(x, y) + V\Psi(x, y) = E\Psi(x, y). \quad (1)$$

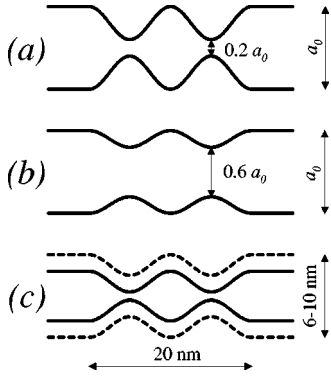


FIG. 1. The width of the wire is always parametrized as $a(x) = a_0 - a_1 \sin^2 2\pi x/a_2$. (a) Weaker coupling: $a_1 = 0.8a_0$ and $a_2 = 2a_0$. (b) Stronger coupling: $a_1 = 0.4a_0$ and $a_2 = 2a_0$. (c) Shape of the ‘‘dot’’ fixed with $a_1 = 5$ nm, $a_2 = 20$ nm, and various wire thickness $a_0 = 6 - 10$ nm.

Here the electron effective mass m^* is chosen to be that of GaAs, equal to 0.067 times the free-electron mass and E is electron energy relative to the conduction-band edge in the wire.

The wave function is expanded in elementary modes or channels,¹⁶

$$\Psi(x, y) = \sum_n \Phi_n(x, y) \psi_n(x), \quad (2)$$

where the basis functions $\Phi_n(x, y)$ are orthogonal solutions of one-dimensional Schrödinger equations in the y direction for fixed x , with eigenenergies $E_n(x)$.

Substituting the expansion Eq. (2) into the Schrödinger equation Eq. (1) leads to a set of ordinary linear differential equations for the channel n wave function $\psi_n(x)$,

$$\begin{aligned} \frac{d^2 \psi_n(x)}{dx^2} + k_n^2(x) \psi_n(x) \\ = \sum_m \left[b_{nm}(x) \frac{d\psi_m(x)}{dx} + a_{nm}(x) \psi_m(x) \right], \end{aligned} \quad (3)$$

where $k_n^2(x) = 2m^*[E - E_n(x)]/\hbar^2$ and

$$\begin{aligned} a_{nm}(x) &= - \int \Phi_n(x, y) \frac{\partial^2 \Phi_m(x, y)}{\partial x^2} dy, \\ b_{nm}(x) &= -2 \int \Phi_n(x, y) \frac{\partial \Phi_m(x, y)}{\partial x} dy. \end{aligned} \quad (4)$$

For the geometry considered here, there are no real bound states in the x direction; only scattering states are relevant.

Zero temperature conductance is calculated using the Landauer formula,^{17,18}

$$G = G_0 \mathcal{T}(E), \quad (5)$$

where $G_0 = 2e^2/h$ and E is here the Fermi energy of the electrons in the leads. The transmission probability $\mathcal{T}(E)$ is the sum of transmission probabilities for all channels, n , at energy E , i.e.,

$$\mathcal{T}(E) = \sum_n \mathcal{T}_n(E), \quad (6)$$

where

$$\mathcal{T}_n(E) = \sum_m |t_{nm}(E)|^2 \quad (7)$$

and $t_{nm}(E)$ is the transition amplitude for scattering from channel n to channel m .

At finite temperatures the conductance is calculated using a generalized Landauer formula,¹⁹

$$G = G_0 \int_{-\infty}^{V_0} \mathcal{T}(\epsilon) \left[- \frac{\partial f(\epsilon - E, T)}{\partial \epsilon} \right] d\epsilon, \quad (8)$$

where $f(\epsilon, T) = [1 + \exp(\epsilon/k_B T)]^{-1}$ is the usual Fermi function. This form is also based on the assumption that motion within the wire is ballistic, the effect of temperature being merely to change the energy distribution in the leads, thus allowing electrons above and below the Fermi energy to contribute to the conductance. For narrow wires, the tail of the Fermi distribution with energy $\epsilon > V_0$ can be significant and the contribution of these electrons to conductance will depend on the size and properties of the barrier region. If this region is large, then electron motion will be diffusive and may be described by an effective conductivity, proportional to δn , the number of electrons in the Fermi tail. The conductance due to these electrons will be further inhibited by rough-surface scattering for mesa structures produced by etching.²⁰ In this paper we shall only consider the conductance due to electrons within the wire by introducing an energy cutoff at $\epsilon = V_0$, as shown in Eq. (8). Thermally activated electrons in the barrier region, which give rise to a series conductance, will be considered in future work.

As pointed out in Ref. 11, the Schrödinger equation Eq. (1) and the expression for conductance, Eq. (8), are invariant under the scaling transformation,

$$\begin{aligned} x, y &\rightarrow \lambda x, \lambda y, \\ E, V &\rightarrow \lambda^{-2} E, \lambda^{-2} V, \end{aligned} \quad (9)$$

$$T \rightarrow \lambda^{-2} T.$$

To solve the system of differential equations, Eq. (3), we first fix the number of channels, N , and then determine the eigenfunctions $\Phi_n(x, y)$ with corresponding eigenenergies $E_n(x)$ for $n \leq N$. N must, of course, be sufficiently large to ensure convergence. For narrow wire this poses a problem since channels with energy above the barrier, V_0 , form a quasicontinuum, and because of interchannel coupling [cf. terms on the right-hand side of Eq. (3)] these high-energy channels can have a significant effect on the eigenstates of electrons confined to the wire. This may be understood in a perturbation theoretic sense. An electron in state $\psi_n(x)$ with $E_n(x) < V_0$ may make a virtual transition to a state $\psi_m(x)$ in the continuum ($E_m > V_0$) and such transitions become very important for $V_0 - E_n$ small, i.e., for confined states close to the top of the barrier. These excursions into the quasicontinuum enhance deconfinement into the classically forbidden regions. This is particularly important near narrow constrictions.

tions, such as the “necks” in Fig. 1(a). The main effect of this, and the leakage of the base states ψ_n into the barrier region, is to broaden resonances compared to cases with $V_0 = \infty$, considered in Ref. 11. To model the quasicontinuum we introduce infinite barriers at $y = \pm L/2$. The basis functions $\Phi_n(x, y)$, x -fixed, are the simple standing waves. Some care is needed in optimizing N and L to ensure convergence. L must be made sufficiently large to ensure that the effect of infinite barriers on the confined wave functions is negligible. On the other hand, L cannot be made too large, otherwise the number of required channels with $E > V_0$ becomes impractical. For the cases we considered, $L \leq 20a_0$ and $N \leq 30$ were sufficient to ensure convergence. The analytic expressions for the functions $\Phi_n(x, y)$ enable the coefficients $a_{nm}(x)$ and $b_{nm}(x)$ in Eq. (3) to be computed efficiently. The system of differential equations Eq. (3) belongs to a class of “stiff” equations for which direct integration is generally not stable. The basic problem is exponentially increasing solutions with imaginary wave vectors of different orders of magnitude leading to round-off errors and divergent results. This problem was solved for the present system by dividing the wire along the x direction in M sections. For each section we first determined $2N$ independent solutions using the fifth-order Runge-Kutta numerical method. The length of each section was chosen to ensure stable numerics in that section, the limiting factor being the number of channels with imaginary $k_n(x)$. In our case up to 10 such channels were taken into account within each section, with $M \leq 10$ sections. Matching the solutions at each boundary yields sets of linear equations from which the transition amplitudes $t_{nm}(E)$ may be determined.

III. RESULTS

Figure 2(a) shows electron conductance at $T=0$ versus energy for the dot geometry of Fig. 1(a), i.e., $a_1 = 0.8a_0$ and $a_2 = 2a_0$ for wire widths a_0 from 4 nm to 20 nm and the barrier height $V_0 = 0.4$ eV. The open circles, \circ , in this and the remaining figures correspond to a Fermi energy $E = V_0$. As explained in the preceding section, electrons with energy greater than this are not “bound” to the wire and their conductance will be dominated by the properties and size of the barrier region. For convenience of presentation and to emphasize the effects of scaled units of energy, we choose scaled units of energy, E/E_0 , where $E_0 = \hbar^2/(2m^*a_0^2)$, the ground-state energy for an electron in a one-dimensional well of width a_0 with infinitely high potential walls. For perfect confinement ($V_0 = \infty$), the scaling invariance, Eq. (9), at $T=0$ gives

$$G(\lambda a_0, E/E_0(\lambda a_0)) = G(a_0, E/E_0(a_0)) \quad (10)$$

and hence all wires of the same shape have identical conductance curves for $V_0 = \infty$.¹¹ This universal curve is approximately that for $a_0 = 20$ nm in Fig. 2(a) (for which the finite barrier height is irrelevant). We note that the (first) resonance occurs at $E \sim 2.5E_0$, which may be interpreted approximately as a resonant bound state with energy E_0 due to confinement in the y direction and energy $1.5E_0$ due to quasiconfinement in the x direction.

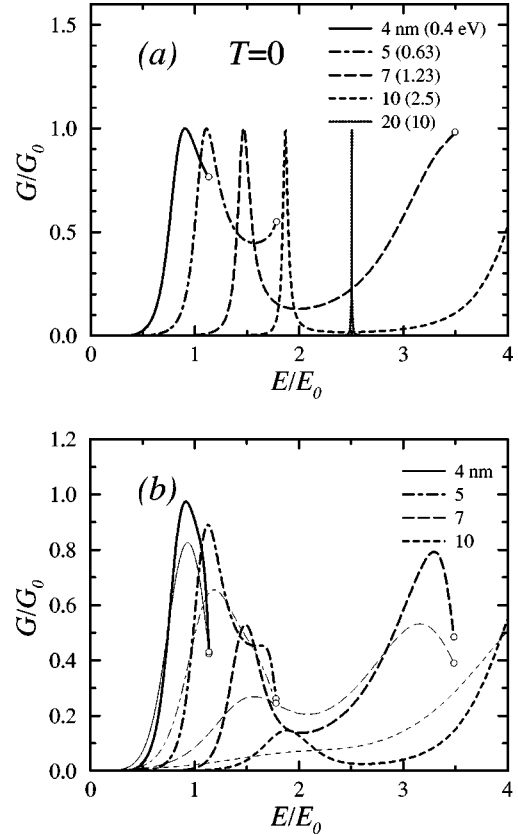


FIG. 2. (a) $T=0$ conductivity [geometry from Fig. 1(a)] for various $a_0 = 4 - 20$ nm and fixed $V_0 = 0.4$ eV (or, equivalently, with fixed $a_0 = 4$ nm and various $V_0 = 0.4 - 10$ eV). (b) Conductivity at $T = 100$ K and 300 K presented with thick and thin lines, respectively, for fixed $V_0 = 0.4$ eV and various $a_0 = 4 - 10$ nm. Circles \circ represent upper limit $E = V_0$ of calculation.

We see that the effect of finite V_0 is to shift the position of the first resonance to lower energies with decreasing wire width. This is, of course, due directly to the deconfinement effect of a finite band offset. For very narrow wires the resonant level is pushed towards the continuum (i.e., unbound in 2D) at energy $E = V_0 = 0.4$ eV and only one resonant level is possible. This is seen to be the case for wires of width 4, 5, and 7 nm. The corresponding energies from the peak to the continuum are 83, 151, and 232 meV for these wires. For wider wires the energy splitting between the first two peaks reduces in energy, eventually decreasing like a_0^{-2} (approximately). Furthermore, the resonances always become broader with decreasing wire width, again a consequence of the deconfinement effect of finite band offset. Thus, at zero temperature, multiple resonances with the highest resolution (ratio of resonance separation to resonance width) occur for wide wires, the limiting resonance width being determined by the geometry (strength of the effective tunnel barriers into the confined region). However, the absolute energy scale is, of course, very small and these sharp resonances are rapidly broadened with temperature. This is shown in Fig. 2(b), where for the same wires we plot conductance at $T = 100$ K and 300 K with thick and thin lines, respectively. Open circles \circ again represent an energy cutoff $E = V_0$, above which conduction is primarily through the barrier region. The thermal broadening is accompanied by a reduction in the

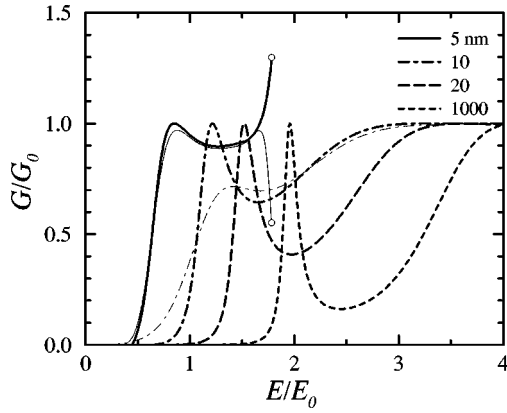


FIG. 3. $T=0$ conductivity [geometry from Fig. 1(b)] for various $a_0=5-1000$ nm and fixed $V_0=0.4$ eV is presented with thick lines. Thin lines represent the corresponding $T=100$ K result. Circles \circ represent upper limit $E=V_0$ of calculation.

peak heights, which are barely resolvable at room temperature for wires with $a_0 > 10$ nm, though clearly resolvable and optimum for $a_0 \sim 5$ nm. This is significantly better than the 4 nm width wire for which the proximity of the continuum has a large effect.

Because of the invariance under scaling, Eqs. (9), the same behavior occurs for larger wires with a smaller band offset, though the overall energy scale is lower. Thus Fig. 2(a) may be regarded as a plot of conductance for wires with the *same* width (4 nm in this case) but *different* band offsets, V_0 . Increasing V_0 increases the confinement and has the same effect as increasing the wire width with fixed V_0 and vice versa, apart from an overall change in energy (temperature) scale. Indeed, the effects of deconfinement could be investigated experimentally for relatively large wires by fabricating quasi-2D wires with small conduction-band offsets. The quasi-2D behavior would be achieved by ensuring high confinement in the third dimension. The behavior of such wires at low temperatures, i.e., conductance versus energy (gate voltage) for various widths, would be the same as that of narrow wires at higher temperatures. This assumes very clean wires and parabolic bands. In practice, one would have to take into account nonparabolicity effects for very narrow wires and the effects of disorder would become increasingly important for larger wires.

In Fig. 3 we show conductance plots at absolute zero and $T=100$ K for the more weakly confining wire of Fig. 1(b), for which $a_1=0.4a_0$ and $a_2=2a_0$. The behavior is seen to be qualitatively similar to the more strongly confined geometry wire, though the resonances are broader, reflecting the weaker confinement along the wire (smaller effective tunneling barriers). However, the thermal broadening is still largely governed by the overall wire thickness. For example, if we compare the 5 nm wires in Fig. 2(b) and Fig. 3 at $T=100$ K (thin lines), we see a similar relative increase in the half-width and a decrease in the peak height compared with absolute zero. This shows that even for small thickness fluctuations, resonance peaks can persist to quite high temperatures for narrow wires.

Finally, we consider the effect of reducing only the thickness of a quantum wire, a_0 , while otherwise maintaining the same shape, $a_1=5$ nm and $a_2=20$ nm, as shown in Fig.

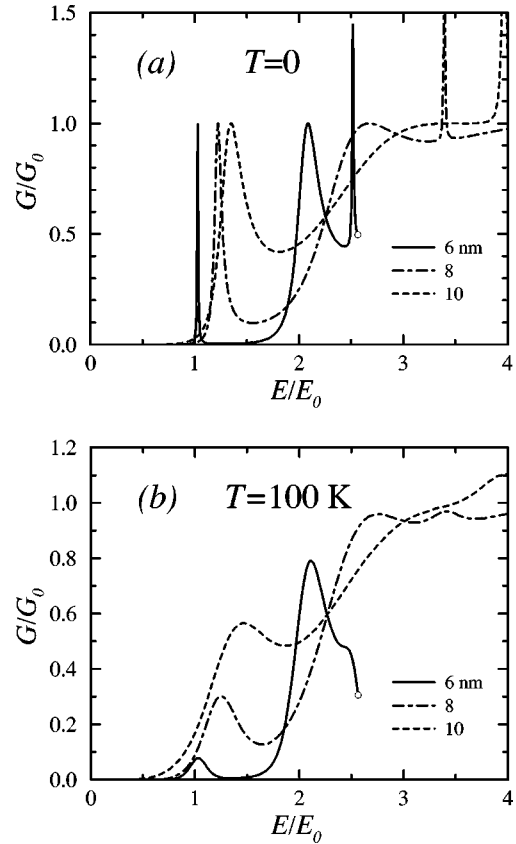


FIG. 4. (a) $T=0$ conductivity [geometry from Fig. 1(c)] for various $a_0=6-10$ nm and fixed $V_0=0.4$ eV. (b) Conductivity at $T=100$ K and the same geometry. Circles \circ represent upper limit $E=V_0$ of calculation.

1(c). This has the effect of producing a quasi-1D quantum dot. There are two competing effects as the wires are made narrower: the effective tunnel barriers increase and there is enhanced deconfinement near the necks. It turns out that the increase in effective tunnel barriers is the greater effect, resulting in sharper resonances as the wire thickness is reduced, as shown in Fig. 4(a). This should be contrasted with Fig. 2(a), which always gives rise to a resonance broadening when the overall size is reduced. However, we point out that, unlike the case of thick wires, this reduction in linewidth is significantly less than that given by a single-channel approximation. This is because there is coupling to the 2D continuum near the neck region. This coupling depends on both the rate of narrowing of the wire and its absolute width. The other main effect shown in Fig. 4(a) is the appearance of further resonance peaks below the continuum. This reflects the quasi-1D nature of the confinement region, the higher-lying peaks corresponding to higher harmonics along the length of the effective quantum dot. Their separation is set by the length of the confinement region along the wire. Conductivity at finite temperature $T=100$ K is plotted in Fig. 4(b). We see that for the wire thicknesses considered, the higher harmonics broaden rapidly with increasing temperature, merging into the quasi-2D continuum. However, it can be seen that the lowest resonance remains distinct.

IV. CONCLUSIONS

With realistic conduction-band offsets, the lowest resonance peak for ballistic transport through quantum wires of

fluctuating thickness giving rise to a quasiquantum dot should be discernible around room temperature for the smallest structures close to the limits of present fabrication techniques. Nevertheless, deconfinement effects due to finite band offsets are significant and ultimately the limiting factor for sufficiently small structures. In principle, the resonances could be made to survive to higher temperatures if heterojunctions could be fabricated with even larger band offsets. The restriction to 2D in the simulations is somewhat artificial here, although the extension to true 3D with circular cross-section wires is feasible and calculations are in progress to estimate the expected enhanced deconfinement effect that they would produce. However, the general behavior is expected to be similar to that described in this paper. Other geometries, such as might be produced from a self-organized

quantum dot connected to source and drain contacts “vertically” is also expected to behave in a similar fashion, although there would be quantitative differences of course. Future work will consider other effects that become increasingly important for very small structures, including nonparabolicity and Coulomb blockade, particularly the effect of deconfinement on the latter.

ACKNOWLEDGMENTS

We acknowledge valuable discussions with Colin Lambert. This work was partly funded by the EU (Contracts ERB CIBD CT940017 and CHRX-CT93-1036). One of the authors (A.R.) would like to thank DERA for the hospitality which was extended to him during his several visits.

-
- ¹W. R. Tribe *et al.*, Appl. Phys. Lett. **70**, 993 (1997).
²J. M. Moison, F. Houzay, F. Rarthe, L. Leprince, E. André, and O. Vatel, Appl. Phys. Lett. **64**, 196 (1994).
³J.-Y. Marzin, J.-M. Gérard, A. Izraël, D. Barrier, and G. Bastard, Phys. Rev. Lett. **73**, 716 (1994).
⁴M. Grundmann *et al.*, Phys. Rev. Lett. **74**, 4043 (1995).
⁵M. Grundmann, O. Stier, and D. Bimberg, Phys. Rev. B **52**, 11 969 (1995).
⁶M. J. Steer *et al.*, Phys. Rev. B **54**, 17 738 (1996).
⁷D. Leonard, K. Pond, and P. M. Petroff, Phys. Rev. B **50**, 11 687 (1994).
⁸M. Walther, E. Kapon, D. M. Hwang, E. Colas, and L. Nunes, Phys. Rev. B **45**, 6333 (1992).
⁹M. Grundmann *et al.*, Semicond. Sci. Technol. **9**, 1939 (1994).
¹⁰R. Rinaldi *et al.*, Phys. Rev. Lett. **73**, 2899 (1994).
¹¹K. Nakazato and B. J. Blaikie, J. Phys.: Condens. Matter **3**, 5729 (1991).
¹²H. Kasai, K. Mitsutake, and A. Okiji, J. Phys. Soc. Jpn. **60**, 1689 (1991).
¹³E. Tekman and P. F. Bagwell, Phys. Rev. B **48**, 2553 (1993).
¹⁴S. A. Gurvitz and Y. B. Levinson, Phys. Rev. B **47**, 10 578 (1993).
¹⁵J. U. Nöckel and A. D. Stone, Phys. Rev. B **50**, 17 415 (1994).
¹⁶A. Szafer and A. D. Stone, Phys. Rev. Lett. **62**, 300 (1989).
¹⁷R. Landauer, IBM J. Res. Dev. **1**, 223 (1957); **32**, 306 (1988).
¹⁸M. Büttiker, Phys. Rev. Lett. **57**, 1761 (1986).
¹⁹P. F. Bagwell and T. P. Orlando, Phys. Rev. B **40**, 1456 (1989).
²⁰Z. Tešanović, M. V. Jarić, and S. Maekawa, Phys. Rev. Lett. **57**, 2760 (1986).